JOURNAL OF CATALYSIS 93, 430–441 (1985)

Oxygen Adsorption on Silver in Polyfluorocarbon Sulfonic Acid (Nafion) Films

GEORGIOS D. CHRYSSIKOS,* VINCENT D. MATTERA, JR.,* WILLIAM M. RISEN, JR.,*,[1] AND ANDREAS T. TSATSAS†

*Department of Chemistry, Brown University, Providence, Rhode Island 02912; and †Inorganic Chemistry Laboratory, Athens University, Athens, Greece

Received August 3, 1984; revised January 18, 1985

The reduction and subsequent oxidation of Ag(I)-containing films of polyfluorocarbon sulfonic acid (Nafion) have been studied spectroscopically, electron microscopically, and kinetically. The ultraviolet–visible and infrared spectral features observed *in situ* during these processes are interpreted in terms of the formation of Ag particles and their surface oxidation upon exposure to air or oxygen. The particle size distributions are narrow and give average diameters of 20–30 Å for various reductive and oxidative treatments. The kinetics of the oxidation, which were followed by observing the growth of silver–silver oxide charge transfer absorption at 370 nm, are analyzed in terms of two parallel reactions. The first, postulated to give atomically adsorbed oxygen, is about 10 times faster than the postulated slower formation of molecularly adsorbed oxygen.

INTRODUCTION

The formation and reactions of small particles of metals such as Ag are of both practical and theoretical interest. In many ways they are intermediate between single atoms and bulk metals and often exhibit size-dependent catalytic properties. For practical reasons such particles usually are studied after being deposited by chemical methods or by vapor deposition techniques on appropriate substrates. However, even when they are deposited very carefully, they can be changed by the sintering that occurs at temperatures above the temperature of preparation (*1*). Thus, it is of interest to study the formation and reactions of metal particles in a medium that can influence or control the size of the particles as well as provide a sufficiently stable and dispersive environment for them to function catalytically.

A class of ionic polymers (ionomers), whose thermodynamic properties favor a morphology capable of exerting particle size control has been developed recently. When the concentration of their ionic sites is high enough, these ionomers can microphase-separate into hydrophobic and hydrophilic phases. The latter are ionic domains embedded in the former. Such materials as sulfonated linear polystyrene (PSSA) and polyfluorocarbon sulfonic acid (PFSA) belong to this class of ionomers. The latter, PFSA, which is known commercially as the DuPont product Nafion, is an ionomer with sulfonate anionic groups at the ends of fluoroether chains that are pendant from a perfluorocarbon polymeric backbone. It is represented by

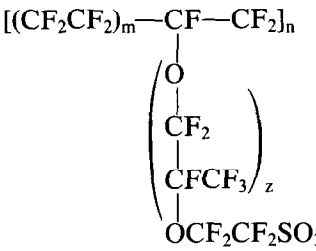

The morphology of PSFA ionomers has been studied by a variety of diffraction (SAXS, WAXS) (*2*, *3*), spectroscopic (*4*,

[1] To whom correspondence should be addressed.

0021-9517/85 $3.00

5), and other techniques, and is believed to be well described as a microphase-separated structure in which the sulfonate groups form in ionic domains that are embedded randomly in a fluorocarbon matrix. The ionic domains vary in size with the degree of hydration and the ionic site concentration, but typically they are about 40 Å in diameter and are connected by hydrophilic channels of about 10 Å diameter (*3*). Theoretical studies on these materials are consistent with the experimental results and suggest that the formation of the site-connecting channels is slightly exothermic (*6*) so that the ionic domains can become isolated at elevated temperature.

In principle, these morphological properties of ionomers can control the size of the metal particles that are formed in the ionic domains. We have confirmed that this occurs in the case of Rh, Ru, and Pt particles that are prepared by reducing their ionomer-supported complex ions (*7, 8*). Silver particles also have been prepared in PFSA (*9*).

The formation and oxidation of Ag particles are of particular interest because of their importance in catalytic oxidation reactions (*10*). There have been many studies of O_2 adsorption on specific planes of Ag crystals, and considerable progress has been made in understanding the reactions involved (*11*). Although less is known about the mechanisms of O_2 adsorption on small silver particles, a great deal of work has been devoted to the problem (*12*). The possibility of contributing with a system of controlled size particles has lead us to investigate the generation of silver particles in PFSA and their subsequent reaction with oxygen.

It is well known that small Ag particles have optical absorption bands in the visible region due to excitation of plasmon modes of the metal (*13*). For silver clusters in the 10-Å-size range, this absorption occurs in the spectral region 350–400 nm. This makes it possible to study the process of forming Ag metal from Ag^+ cations in the domains of the nearly transparent Ag–PFSA ionomer films. The oxidation can be followed as well. Molecular orbital calculations on models of oxidized silver particles predict that charge-transfer transitions of such species as ($Ag–Ag^+$) and ($Ag–Ag^+–O$) will occur in the visible region, so optical absorption due to surface oxygen species is also to be expected in this region (*14*). The presence of these bands makes it possible to measure the rates of oxidation precisely enough to obtain data to which a kinetic model of the processes can be applied. That has been done in this work.

The PFSA films have several other advantages in addition to exerting particle size control and being sufficiently transparent to allow the formation and oxidation of Ag particles to be studied spectroscopically. On advantage is that any reduction of Ag^+ to Ag must change the counterions at the anionic sites in a manner that allows the process to be followed independently by infrared spectroscopy. Another advantage is that the bulk material can be studied by electron microscopy using standard sectioning methods so that the size and shape distribution of the particles can be determined.

In this paper, we report our study of the formation and oxidation of Ag particles in a PFSA medium.

EXPERIMENTAL

The PFSA ionomer films employed to isolate silver in this study have an equivalent weight of 1600, and an approximate thickness of 25 μm which is convenient for study by UV–visible and transmission infrared spectroscopy. The materials are of the type known as Nafion, and were kindly provided by the Plastics Department of the E. I. DuPont de Nemours Corporation.

Prior to ion exchange, ca. 5-cm^2 sections of the ionomer film were purified to remove plasticisers and salts and treated with acid to transform them completely into the H^+ form. Thus, they first were stirred for 30 min in a 5 *M* nitric acid aqueous solution

and rinsed with distilled water, then they were stirred for 30 min in dimethyl sulfoxide (DMSO, analytical grade), and rinsed thoroughly again with distilled water. Silver ions were incorporated into the PFSA by stirring the films in a 0.05 *M* aqueous silver nitrate solution ($AgNO_3$, analytical grade, Mallinckrodt) for 30 min at room temperature. The partially hydrated films were then rinsed with distilled water and allowed to dry in air prior to storing them in a dessicator.

Membranes prepared in this manner were analyzed by the Galbraith Laboratories, (Knoxville, Tenn.), and were shown to contain 1.76 wt% sulfur and 4.81 wt% silver. This corresponds to approximately 80% completion of the ion exchange.

The hydrogen used in this work (99.995% H_2, Airco, Inc.) was purified further by passing it through a series of liquid-nitrogen traps upon its addition to the spectroscopic cell. The cell, which consists of a Pyrex body to which infrared (KBr) or UV–visible (SiO_2) transmitting windows are affixed with a cyanoacrylate glue, could be connected to a vacuum or gas supply line. The sample holder was machined from a PTFE block and could be aligned with the KBr or SiO_2 windows. Using this cell, the spectra were taken *in situ* of films subjected to various treatments. During hydrogen reduction and spectral acquisition, the cell was covered with aluminum foil to exclude light. The subsequent oxidation of the silver particles formed by the H_2 reduction was carried out by admitted air or dry oxygen to the cell.

The infrared spectra in the region 3800–400 cm^{-1} were recorded at 300 K with a Digilab 15B FT-IR spectrometer. Each trace is the average of 400 scans and represents a spectrum recorded at 2 cm^{-1} resolution. The UV–vis spectra in the region 700–300 nm were recorded at 300 K with a Cary 17 UV-VIS–near-IR spectrophotometer at 1 nm resolution.

Transmission electron microscopy (TEM) was used to investigate the silver-containing PFSA membranes after the H_2 reduction treatment and exposure to air. Samples were prepared for TEM by embedding the films in Spurr's low-viscosity embedding medium, (Electron Microscopy Sciences, Fort Washington, Pa.) and microtoming them into section 60–70 Å thick. These sample sections, which were supported on Cu grids, were examined using a Philips Model 410 LS transmission electron microscope. As operated at 100 kV in the bright field mode at calibrated magnification of 500,000×, the instrument is capable of resolving features that are ca. 3.5 Å in diameter.

Electron microprobe analysis (EDAX) was performed on the PFSA–Ag membranes, (after hydrogen treatment and exposure to air), using an EDAX Model 711 instrument interfaced to an AMR 1000 scanning electron microscope. The analyses were performed using the low-energy secondary electron imaging mode.

RESULTS AND DISCUSSION

The reduction of Ag(I) ions in the ionic domains of PFSA–Ag(I) films with H_2, and the subsequent adsorption of O_2 on the reduced Ag-containing material have been studied spectroscopically. Separation of these processes has made it possible not only to identify the optical absorption due to H_2-reduced Ag–PFSA, but also to follow the oxidation kinetics. In the first part of this section the reduction and oxidation are presented, and in the second part the kinetics of the oxygen adsorption processes are analyzed.

Reduction and Oxidation of Ag Species in PFSA

In order to determine the visible spectrum of the reduced Ag–PFSA films and make it possible to study the adsorption of O_2 on the reduced silver species, the ultraviolet–visible spectra were recorded in the region 300–700 nm as the reduction proceeded. The spectrum of PFSA–Ag(I), before reaction, is shown in Fig. 1a. The only

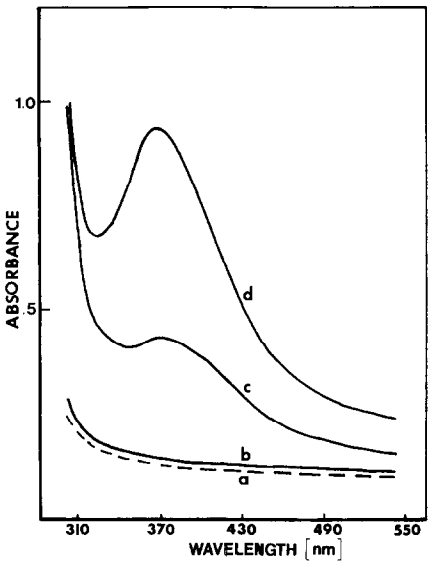

FIG. 1. Visible spectra of PFSA–Ag(I) upon exposure to H_2: (a) at zero exposure, (b), (c), and (d) after 14, 19, and 24 h of reduction, respectively.

spectral feature is a baseline absorption which rises as the wavelength decreases. This is characteristic of the PFSA support itself and does not indicate any additional scattering or absorption associated with the presence of Ag^+ ions in the domains. Thus, neither hydrated Ag^+ nor Ag^+ associated with sulfonate and H_2O moieties give rise to absorption in this region.

During exposure of such a film to H_2 at 1 atm and 300 K, the spectrum changes slowly as the films turn yellow and absorbance bands grow in the region 300–400 nm. This is shown in Figs. 1b, c, and d, which are the spectra observed after exposure to H_2 for 14, 19, and 24 h, respectively. After 24 h of treatment with H_2, the spectrum displays an asymmetric band envelope with a peak at 365 nm.

The growth of this band clearly correlates with the reduction process. Since this reduction requires production of Ag^0 and since the other product, Ag^+-containing hydrated H–PFSA, does not have absorption bands in this region, the absorption must be associated with Ag^0. Two general types of apparent optical absorption that depend on the presence of Ag^0 can be considered. One involves the interaction of light with Ag^0 particles themselves, presumably through collective electronic excitations (plasmon modes), or, at relatively large spacings, through interparticle scattering. The other involves electronic excitations between states that have important contributions from the electronic structure of Ag^0 particles but also include contributions in the ground and/or excited state from neighboring or bound atoms or ions of another type. Since there is no noticeable change in the visible absorption until after significant reduction has occurred, as shown by the infrared spectrum (vide infra), it appears that the Ag^0 particles must grow to a minimum size before they cause the band to appear.

Investigations of the concentration dependence of the optical properties of Ag^0 clusters isolated in rare-gas matrices show that a broad asymmetric absorption occurs at about 360 nm when the clusters reach about 10 Å in diameter (*15, 16*). For Ag^0 particles of about 100 Å diameter deposited on glass slides, Granqvist *et al.* observed a similar absorption at 375 nm (*17*). Doremus found that ca. 100 Å Ag^0 particles in inorganic glasses absorb at about 400 nm (*18*). For particles with a range of sizes in yellow aqueous colloidal suspensions of silver, Creighton found an absorption band at ca. 385 nm (*19*). Finally, Lee and Meisel found an asymmetric absorption band at ca. 375 nm in reduced Ag–PFSA membranes that had been prepared by bubbling H_2 over a PFSA–Ag(I) film at 333 K in water that had been deoxygenated to prevent the oxidation that occurred upon exposure to air (*9*). Since the plasmon absorption of Ag^0 particles in the diameter range 10–100 Å occurs in the region 350–400 nm in a variety of environments, we tentatively assign the 365-nm band to this absorption by the Ag^0 particles formed as the PFSA–Ag(I) films were reduced in this work.

Even though this assignment appears to apply to Ag^0 particles even in significantly different environments, it still is possible,

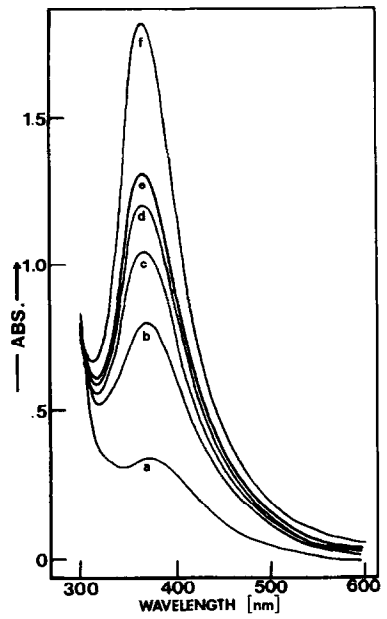

FIG. 2. Visible spectra of reduced PFSA–Ag^0 exposed to air for (a) 0, (b) 10, (c) 20, (d) 30, (3) 40, and (f) 500 min. This sample was exposed to H_2 for 19 h.

in principle, for the ground or excited state to have a contribution from species associated with the Ag particles. Nonetheless, the Ag particles are a necessary component of the absorbing species.

Following reductions of the PFSA–Ag(I) films for periods of 9, 14, 19, 23, and 24 h, the films were exposed to air at 300 K. Two types of experiments were done on them. First, the ultraviolet–visible spectra and the infrared spectra were measured as oxidation proceeded, and, second, sections of each film were measured by transmission electron microscopy (TEM) to determine the particle size distribution of the oxidized product.

Upon exposure to air, the reduced-silver–PFSA films develop a bright golden yellow color, and their spectra show that an absorption band at ca. 370 nm grows dramatically. Spectra representing the time evolution of this band in the case of a film first reduced for 19 h under H_2 are shown in Fig. 2. In Fig. 3, the absorbance at 370 nm, A_{370}, is plotted versus time of exposure to air for all five of the initial reduction times. The data for films reduced for 30 h before oxidation constitute the limiting case because of the very high absorbance values they attain quickly when exposed to air.

In order to follow this oxidation process, as well as the initial reduction, independently, the infrared spectra of the films were monitored through the processes. Since the absorbance changes represent transformations of each film from one that is essentially hydrated PFSA–Ag(I) with some H–PFSA to one that contains Ag^0, less of the hydrated PFSA–Ag(I) and more H–PFSA, when it is reduced, and then to one that contains less Ag^0 and, at least, more H_2O, the changes are less dramatic than those seen in the visible spectrum. Nonetheless, they are important in showing independently that these processes occur. The most useful region to focus on is that between 1600 and 1900 cm^{-1}, because it contains the bending mode of H_2O that is sensitive to the type and amount of cation present. Thus, H_2O associated with Ag^+ ab-

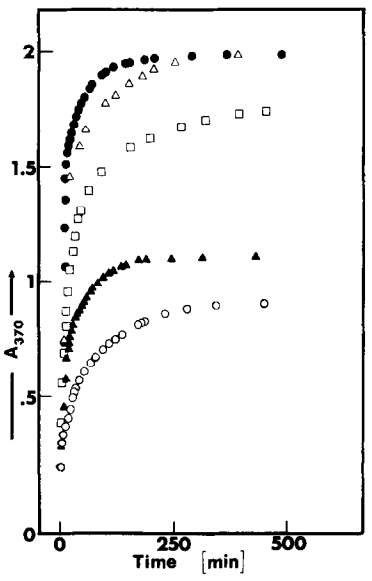

FIG. 3. The time evolution of absorbance (at 370 nm) exhibited by PFSA–Ag^0 films exposed to air. The different curves correspond to membranes prepared after (▲) 9, (○) 14, (□) 19, (△) 23, and (●) 24 h of exposure to H_2.

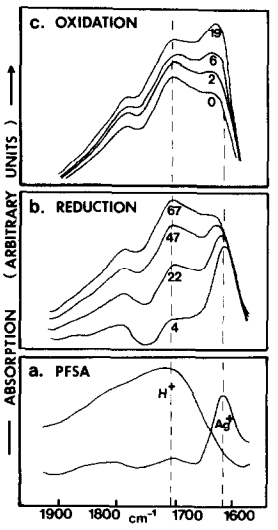

FIG. 4. (a) Infrared spectra of PFSA–Ag^+ and PFSA–H^+ in the water-bending region. (b) Infrared spectra of PFSA–Ag^+ upon H_2 reduction. (c) Infrared spectra of reduced PFSA–Ag upon exposure to air. In (b) and (c), the numbers indicate the number of hours of exposure to H_2 and air, respectively.

sorbs at 1620 cm^{-1} and H_2O associated with H–PFSA absorbs at 1710 cm^{-1}, as shown in Fig. 4a. As the reduction proceeds, the 1620-cm^{-1} band decreases while the 1710-cm^{-1} band increases, as expected when Ag^+ is reduced to Ag^0. This is shown in Fig. 4b, where IR spectra taken *in situ* after 4, 22, 47, and 67 h of reduction are presented. The fact that the 1710-cm^{-1} absorbance reaches the value of the initial 1620-cm^{-1} band after 67 h of treatment with H_2, is required if full reduction occurs and the oscillator strength of H^+-bound H_2O is the same as that of Ag^+-bound H_2O, because the total amount of silver in the film is constant throughout the process. Upon oxidation, this observation is reversed. Thus, when the same film (67-h reduction) has been exposed to air for 0, 2, 6, and 19 h, the relative band intensities reverse as shown in Fig. 4c.

All of the films, which had been reduced for the various periods specified above and then exposed to air, were embedded for TEM measurement. The TEM images were then analyzed to determine the distribution of particle sizes. The TEM image for a material reduced for 24 h before measurement is shown in Fig. 5, and its particle size distribution, obtained by standard statistical counting techniques, is shown in Fig. 6. The average particle size is 29 Å diameter for this film. For each of the Ag–PFSA materials, at all reduction times, the particle size distribution is similar in that it is relatively narrow, peaked in the range 20–30 Å, and gives an averaged particle size of 25 ± 5 Å diameter. Although there are obviously a few larger particles, their statistical weight is too small to be shown in the standard particle size distribution representation. The average particle size reported in this work is considerably smaller than the 70-Å particle size reported by Lee and Meisel on Ag–PFSA that was reduced by bubbling H_2 through water containing thin films (*9*).

The degree of initial reduction achieved naturally depends on the time of treatment with H_2. Even after 67 h of exposure to H_2 under the conditions specified, the reduction is incomplete as shown by the presence of the infrared band at 1620 cm^{-1}, so some Ag^+ remains. The oxidation of Ag^0 particles also is incomplete even after a prolonged exposure to air. To demonstrate this, EDAX experiments were performed on a film which had been reduced for 70 h in H_2 in order to represent a practically limiting case.

The EDAX analysis of this film, after exposure to air for longer than the 10 h it takes for the oxidation to be complete spectroscopically, shows two intense peaks at 3.05 and 2.37 keV corresponding to Ag and S, respectively. The ratio of the areas under the curves reflects the Ag-to-S concentration ratio of the membrane, and, in separate units of unit area per atom, was 1.5. After this film was stirred for 1 h in 5 *M* $HClO_4$, which removes Ag^+ ions, the EDAX analysis showed that the ratio of the Ag-to-S curve areas had decreased to 0.35. Taking a ratio of these curve area ratios eliminates

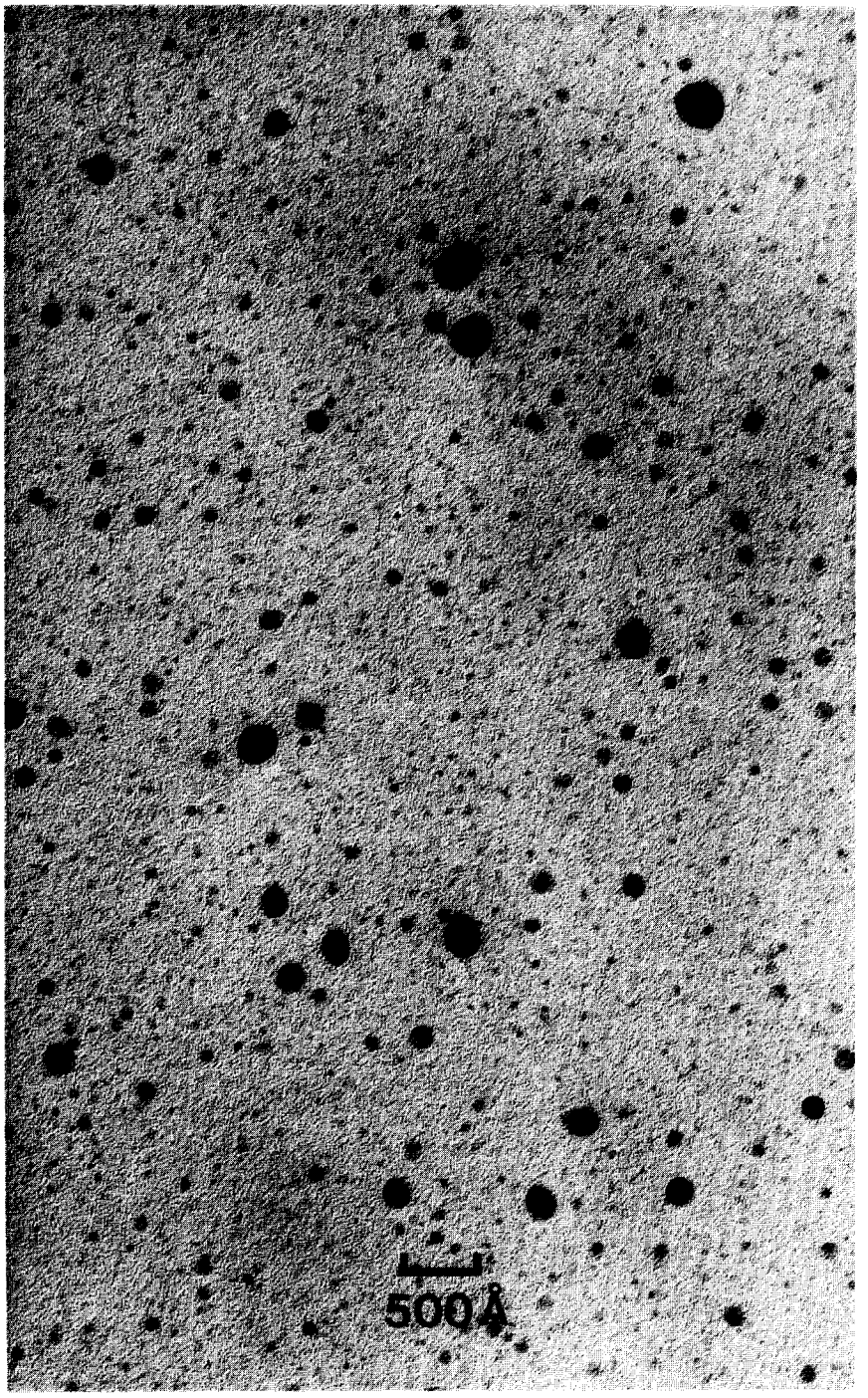

FIG. 5. Transmission electron micrograph of a PFSA–Ag membrane reduced in H_2 for 24 h and exposed to air. It shows particles of 29 Å average diameter.

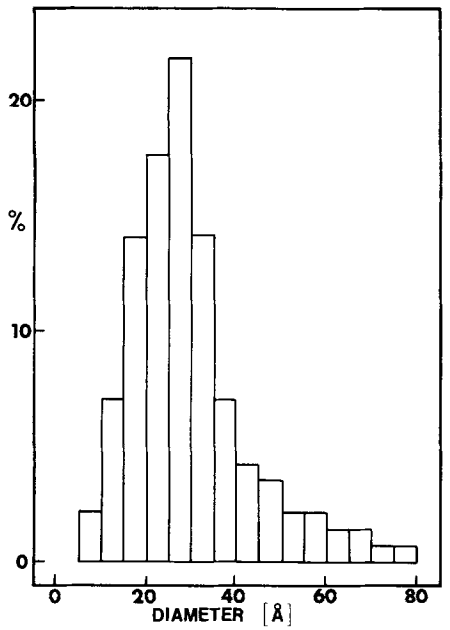

FIG. 6. The particle size distribution resulting from the micrograph shown in Fig. 5.

the differences in units of area per atom and yields a measure of the neutral silver. Thus, after reduction in H_2 for 70 h and subsequent air oxidation, about 24% of the total amount of silver initially exchanged into the film remained as metallic Ag.

The reduction and oxidation experiments on Ag–PFSA thus show that Ag^+ is reduced to Ag^0 to a significant degree and produces particles after oxidation which are about 20–30 Å in size for any degree of reduction studied. The oxidation leads to growth of a strong visible absorption band at 370 nm which is assigned to charge transfer transitions ($Ag–Ag^+–O$) involving Ag^0 and its oxidized surface. The growth of this band occurs on a time scale that makes it possible to measure the kinetics of the oxidation reaction directly.

Kinetics of Oxidation of Reduced Ag-PFSA

The variation with time of the optical absorption due to exposure to air has been measured over a sufficient portion of the reaction to make it possible to model the kinetics of the process. Since the absorption increased and then leveled off in the exponential manner typically observed for oxygen adsorbing on silver (*11, 20–25*), under a variety of experimental conditions, the first approach to modeling was to assume that the rate of the reaction could be expressed as $dA_t/dt = A_\infty K \exp(-kt)$, where A_t is the optical absorbance at time t, A_∞ that at equilibrium, K a constant, and k the rate constant. More directly, in measured quantities, the following rate law was tested:

$$\frac{-d\left(1-\frac{A_t}{A_\infty}\right)}{dt} = k\left(1-\frac{A_t}{A_\infty}\right). \qquad (1)$$

Here, A_t/A_∞ represents the degree of surface oxidation since direct evaluation of a relevant coverage, θ, is not possible. In general, k includes a factor which is postulated to be constant under the condition that the local pressure of O_2 reaches a steady state as in our constant external pressure experiments. The solution to (*1*) is, of course,

$$A_t = A_\infty(1 - e^{-kt}) \qquad (2)$$

or,

$$\ln\left(1-\frac{A_t}{A_\infty}\right) = -kt. \qquad (3)$$

It is possible to obtain a rate expression of the form of (2) or (3) from other models. For example, Clarkson and Cirillo (*22*) treated their data for uptake of O_2 on Ag particles using first-order adsorption and desorption terms for $O^-_{2,a}$ formation on silver upon exposure to constant pressures of O_2. Under their assumptions the solutions is again of the form of Eqs. (2) and (3). The experimental data do not allow discrimination between kinetic rate laws of the same form so no conclusion can be drawn about the rate order of the adsorption/desorption reactions involved in our system. Nevertheless, Eq. (3) is particularly helpful in interpreting the rate data.

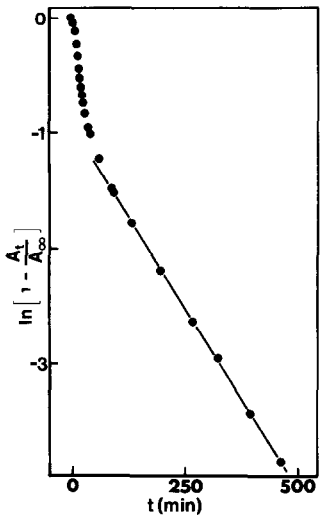

FIG. 7. The $\ln[1 - A_t/A_\infty)]$ versus time for a PFSA–Ag film exposure to air after 19 h of reduction in H_2. Dots represent points calculated from experimental data. The solid line shows the least-squares fitting to a straight line in the long-time scale.

Plots of $\ln[1 - (A_t/A_\infty)]$ versus t, such as that shown in Fig. 7 for the case of a film reduced for 19 h, were obtained and used for the graphical determination of k in Eq. (3). It can be seen that for times greater than ca. 40 min, the agreement is excellent. Least-squares fitting to a straight line gave correlation coefficients of 0.9999 or better in all cases. However, the model fails to predict the first part of the reaction, which apparently involves another faster reaction.

When the curve of the form of Eq. (3) with the value of k that was fit precisely for long times was subtracted from the corresponding experimental curve in each case, the difference was precisely (correlation > 0.999) a second curve of the same form, with a value of k approximately 10 times as great. The two curves, together with the experimental data shown in Fig. 3, are shown in Fig. 8. The fitting of each set of data with two curves of the form of Eq. (3) lead to the same result. In each case there is a constant baseline and, superimposed on it is a curve of the form

$$A_t = A_{\infty,1}(1 - e^{-k_1 t}) + A_{\infty,2}(1 - e^{-k_2 t}). \quad (4)$$

TABLE 1

Values of Parameters of Eq. (4) for the PSFA–Ag^0 Films Studied

Time of reduction (h)	k_1 (s^{-1})	k_2 (s^{-1})	$\frac{k_2}{k_1}$
9	2.8×10^{-4}	3.47×10^{-3}	12.39
14	1.1×10^{-4}	0.85×10^{-3}	7.73
19	1.1×10^{-4}	1.08×10^{-3}	9.82
23	2.0×10^{-4}	2.02×10^{-3}	10.10
24	3.5×10^{-4}	3.42×10^{-3}	9.77
	Average:		9.96

All of the values of k_1 are on the order of 10^{-4} s^{-1} and those of k_2 are about 10^{-3} s^{-1}. They are given in Table 1.

Interpreting these kinetic results raises several interesting questions. The first is whether they are unique. There clearly is an infinite number of mathematical ways to fit any curve, if only by fitting it to an infinite series. However, in the present case the possibilities could be limited by using the linear variation of $\ln[1 - (A_t/A_\infty)]$ with

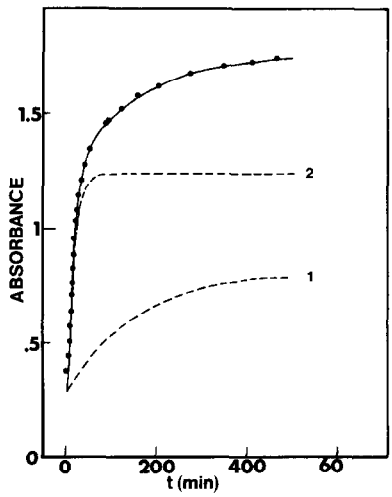

FIG. 8. The deconvolution of the absorbance at 370 nm, A_{370}, versus time of exposure to air plot in the case of a PFSA–Ag^0 membrane prepared for 19 h of H_2 reduction. Dots represent the experimental data shown in Fig. 3. Dashed lines are the deconvoluted slow (1) and fast (2) reaction curves. The sum of these also is shown (solid line).

time, at long times. This permits direct evaluation of k_1. A difference plot between the curve with that determined value of k_1 and the observed curve, leads to a very limited range of values for k_2 if only one additional term is used. The fact that only one is required to obtain a very precise fit is necessary, though recognizedly not sufficient, evidence that this treatment is valid. Reaction processes of this form but with k orders of magnitude smaller than 10^{-4} s^{-1} cannot be evidenced by this approach since they would be too slow to proceed to an appreciable extent on our experimental scale. Processes that are much faster and are completed within the first minute of the experiment, simply contribute to the baseline.

The second question concerns the apparent assumption that both reactions lead to products that absorb light at 370 nm. This is not actually an assumption but a conclusion from the data. The question is, rather, how to rationalize there being two different products that lead to such absorption. As discussed above, the optical absorption is assigned to transitions that transfer charge from Ag^0 to Ag^+. So long as the Ag^0 is in particles that are large enough to have a Fermi level near that of the bulk metal and "Ag^+" has energy levels characteristic of ions that have fully transfered their electron to oxygen in some form, each ($Ag–Ag^+–O$) species is expected to exhibit its charge transfer transition in the range 350–380 nm (*14*). Thus, any of several such species should have appreciable optical absorption at 370 nm.

The next question to be addressed concerns the nature of the species that are formed. The interaction of oxygen with silver has been studied widely over the years largely because of its importance in understanding the catalysis by silver of ethylene epoxidation. Two different types of model experimental systems often are used to study this reaction. One involves polycrystalline silver surfaces exposed to oxygen at relatively high pressures (1–760 Torr). The other involves the reaction of O_2 with clean single crystals of silver at very low exposures and the study of the resulting adsorbates under UHV conditions. Both have been reviewed extensively (*10, 12, 26*), and it is clear that while both are useful the differences in reaction conditions often make comparisons of the two sets of data difficult. Indeed, the nature of the chemisorbed species depends very strongly upon the configuration, pretreatment, and purity of the surface, the temperature of adsorption, the oxygen pressure, and degree of exposure, and the experimental conditions required for the probe experiment.

Uptakes of oxygen in the high-pressure regime (1–760 Torr), were studied volumetrically by Smeltzer *et al.* (*20*), gravimetrically by Czanderna (*23*), and manometrically by Kilty *et al.* (*27*), at temperatures as high as 300 K. Their results are consistent in indicating that there are several adsorption states of oxygen on silver. One is formed in an initial, almost nonactivated step (E_a = 12.5 kJ/mol). It was found in all cases and is thought to involve dissociative adsorption of oxygen (i.e., the formation of adsorbed atomic oxygen). A second state, formed with E_a = 33.4 kJ/mol, is observed after about a half-monolayer coverage. It is thought to be adsorbed but undissociated $O_{2,a}$. At higher temperatures a third, highly activated (E_a = 58 or 92 kJ/mol), adsorption, possibly associated with migration of silver atoms or formation of subsurface oxygen, has been observed.

While there is evidence for at least two species being formed when polycrystalline Ag is exposed to O_2 at high pressures and room temperature (*28–30*), their identities are not based solely on uptake or thermal desorption data. For example, Joyner and Roberts found evidence for atomically and molecularly adsorbed oxygen when polycrystalline Ag foil was exposed to O_2 at 473 K and 1 Torr (*31*). Under those conditions, oxygen adsorbate species exhibited three distinct O(1*s*) binding energies in the high-pressure photoelectron spectrum. In addition, Kilty *et al.* demonstrated the presence

of $O_{2,a}$ under similarly realistic conditions (*27*) through careful infrared studies of isotopically labeled systems.

Perhaps the most direct evidence for a molecular oxygen adsorbate on Ag under realistic conditions is the observation of a paramagnetic O_2^- adsorbate on silver particles (*22, 32–34*). By monitoring the ESR spectrum of oxygen adsorbed on 47-Å mean-diameter silver particles supported on Vycor glass at 1 Torr in the range 298–333 K, Clarkson and Cirillo were able to identify the $O_{2,a}^-$ species and to follow the kinetics of its formation. The rate equation that describes their ESR data is the same as Eq. (3). Taking this result and the fact that the activation energy is known to be 61.7 kJ/mol from both the ESR study and the work of Czanderna (*28*), it is possible to calculate what the rate constant for the formation of this O_2^- species should be under our experimental conditions. That calculated values is 3.5×10^{-4} s^{-1}, in excellent agreement with our value for k_1, the slower adsorption step, obtained in the present study.

On this basis, we can assign the oxygen adsorbate species that lead to the distinct uptake curves shown in Figs. 7 and 8. In agreement with Czanderna (*23*), Kilty *et al.* (*27*), and Clarkson *et al.* (*22*), we assign the faster step as a dissociative one leading to atomically adsorbed oxygen, O_a. The slower step involves nondissociative adsorption of oxygen on the surface of the PFSA-supported silver particles, presumably $O_{2,a}^-$. Subsurface oxygen, observed at higher temperatures by other techniques, is not expected to be probed by UV–vis spectroscopy.

It is reasonable to ask whether the observed peaks are due to contaminant adsorbates, such as CO_2 or H_2O. To investigate this, the oxidation experiments were repeated with dehydrated Ag–PFSA membranes and with dry oxygen, instead of air. The same two adsorbing species were observed.

The formation of the atomic state, O_a, by the faster reaction may be diffusion rate limited. When the oxidation experiments were repeated with dehydrated Ag–PFSA membranes and with oxygen instead of air, the same two absorbing species were observed. This observation of the same species appears also to exclude adsorbed CO_2 or H_2O interferences. However, the rate constant for the fast step was reduced by a factor of 3 to 5. This is consistent with the reduction of the O_2(g) diffusion coefficient expected for PFSA upon dehydration.[2] Diffusion control of other reactions in PFSA supports have been observed in this laboratory. For example, the rates of CO oxidations catalyzed by Ru–, and Rh–PFSA have been shown to be diffusion controlled (*7*). On the other hand, the rate of CO oxidation catalyzed by Pt–PFSA, which is much slower, is not (*8*).

Although the assignments of the two adsorption processes and adsorbates made above are well precedented, it is possible that the two adsorbates do not differ in molecularity. For example, they could be atomic oxygen adsorbed at two different sites, or adsorbed atomic oxygen ad subsurface oxygen. These possibilities are suggested by the fact that the occurrence of many oxygen adsorbates on polycrystalline silver has been attributed to the availability of a variety of sites (*36*). They also are based on the recent report of Campbell and Paffet (*37*), who suggested that their TPD studies of Ag(110) at high exposures of oxygen are best interpreted in terms of the formation of two atomic oxygen adsorbates at high temperatures (ca. 300 K) in addition to the molecular oxygen adsorbate identified by UHV studies (*24, 25, 38*) which desorbs

[2] While the gas diffusion coefficient for dried Nafion ionomers have not been reported, studies on gas diffusion in hydrated Nafions show that $D(O_2) \cong 3 \times 10^{-7}$ cm^2 s^{-1} in the range 290–310 K. Ogumi *et al.* argue that the mechanism of O_2 diffusion in the hydrophobic regions, which dominate in the dried membranes, is close to that of PTFE and therefore should give $D \cong 1 \times 10^{-7}$ cm^2 s^{-1} (*35*). Thus, a roughly two- to fivefold reduction should be expected on the basis of the difference in O_2 diffusion rates.

rapidly above 190 K. However, the existence of molecularly adsorbed $O_{2,a}$ at 300 K and high pressure has been confirmed by ESR, isotopic-exchange infrared, and XPS/UPS studies. This and the fact that UV–visible spectra are not expected to probe subsurface oxygen, lead to the assignment given. Thus, we conclude that the faster process is a diffusion rate-limited formation of atomically adsorbed oxygen and the slower process is a formation of molecularly adsorbed oxygen.

ACKNOWLEDGMENTS

We gratefully acknowledge the partial support of this work and the use of the Central Facilities of the Materials Research Laboratory at Brown University. We are particularly grateful for the assistance of Ms. Sandra Kunz of the Brown Division of Biology and Medicine, and for helpful discussions with Professor P. J. Estrup, Professor D. Katakis, and Mr. S. P. Koinis.

REFERENCES

1. Anderson, J. R., "Structure of Metallic Catalysts," p. 134. Academic Press, New York/London, 1975.
2. Yeo, S. C., and Eisenberg, A., *J. Appl. Polym. Sci.* **21,** 875 (1977).
3. Gierke, T. D., Munn, G. E., and Wilson, F. C., *J. Polym. Sci.-Phys.* **19,** 1687 (1981), and references therein.
4. Falk, M., *Can. J. Chem.* **58,** 1495 (1980).
5. Peluso, S. L., Ph.D. thesis. Brown University, 1980.
6. Hsu, W. Y., and Gierke, T. D., *Macromolecules* **15,** 101 (1982).
7. Mattera, V. D., Jr., Barnes, D. M., and Risen, W. M., Jr., to be submitted for publication.
8. Mattera, V. D., Jr., Noor-Chaudhuri, S., and Risen, W. M., Jr., to be submitted for publication.
9. Lee, P. C., and Meisel, D., *J. Catal.* **70,** 160 (1981).
10. Sachtler, W. M. H., Backx, C., and Van Santen, R. A., *Catal.-Rev.-Sci.-Eng.* **23,** 127 (1981).
11. Engelhardt, H. A., and Menzel, D., *Surf. Sci.* **57,** 591 (1976).
12. Barteau, M. A., and Madix, R. J., *in* "The Chemical Physics of Solid Surfaces and Heterogeneous Catalysis" (D. A. King and D. P. Woodruff, Eds.), Vol. 4, pp. 100–113. Elsevier, Amsterdam, 1982, and references therein.
13. Papavassiliou, G. C., *Prog. Solid State Chem.* **12,** 185 (1979).
14. Schoonheydt, R. A., Hall, M. B., and Lunsford, J. H., *Inorg. Chem.* **22,** 3834 (1983).
15. Schulze, W., Becker, H. U., and Abe, H., *Chem. Phys.* **35,** 177 (1978).
16. Ozin, G. A., and Huber, H., *Inorg. Chem.* **17,** 155 (1978).
17. Granqvist, C. G., Calander, N., and Hunderi, O., *Solid State Commun.* **31,** 249 (1979).
18. Dorenus, R. H., *J. Appl. Phys.* **35,** 3456 (1964).
19. Creighton, J. A., "Surface Enhanced Raman Scattering" (R. K. Chang and T. E. Furtak, Eds.). Plenum, New York, 1982.
20. Smeltzer, W. W., Tollefson, E. L., and Cambron, A., *J. Catal.* **34,** 1046 (1956).
21. Backx, C., Moolhusen, J., Geenen, P., and Van Santen, R. A., *J. Catal.* **72,** 364 (1981).
22. Clarkson, R. B., and Cirillo, A. C. Jr., *J. Catal.* **33,** 392 (1974).
23. Czanderna, A. W., *J. Phys. Chem.* **68,** 2765 (1964).
25. Backx, C., Groot, C. P. M., and Biloen, P., *Surf. Sci.* **104,** 300 (1981).
26. Verykios, X. E., Stein, F. P., and Coughlin, R. W., *Catal. Rev.-Sci.-Eng.* **22,** 197 (1980).
27. Kilty, P. A., Rol, N. C., and Sachtler, W. M. H., *in* "Proceedings, 5th International Congress on Catalysis, Palm Beach, 1972" (J. W. Hightower, Ed.), p. 929. North-Holland/American Elsevier, Amsterdam, 1973.
28. Czanderna, C. A. W., Chen, S. C., and Biegen, J. R., *Chem. Phys. Lett.* **76,** 294 (1980).
29. Kagawa, S., Iwamoto, M., Mori, H., and Seiyama, T., *J. Phys. Chem.* **85,** 434 (1981).
30. Kagawa, S., Iwamoto, M., and Seiyama, T., *CHEMTECH,* 426. July 1981.
31. Joyner, R. W., and Roberts, M. W., *Chem. Phys. Lett.* **60,** 459 (1979).
32. Tanaka, S., and Yamashina, T., *J. Catal.* **40,** 140 (1975).
33. Abou-Kais, A., Jarjoui, M., Vedrine, J. C., and Gravelle, P. G., *J. Catal.* **47,** 399 (1977).
34. Clarkson, R. B., and McClellan, S., *J. Phys. Chem.* **82,** 394 (1978).
35. Ogumi, Z., Takehara, Z., and Yoshizawa, S., *J. Electrochem. Soc.: Electrochem. Sci. Technol.* **131,** 769 (1984).
36. Ekern, R. J., and Czanderna, A. W., *J. Catal.* **46,** 109 (1977).
37. Campbell, C. T., and Paffet, M. T., *Surf. Sci.* **143,** 517 (1984).
38. Sexton, B. A., and Madix, R. J., *Chem. Phys. Lett.* **76,** 294 (1980).